MOF-Ionic Liquid Engineered Polymer Electrolyte for Advanced Solid-State Sodium Metal Batteries

Xilin Luo,[a] Le Zhao,*[b] Shuangwu Xu,[a] Haijun Peng,*[a] Jian Tu,[c] Yougen Tang,[a] and Haiyan Wang*[a]

[a.] Hunan Provincial Key Laboratory of Chemical Power Sources, College of Chemistry and Chemical Engineering, Central South University, Changsha, 410083, P. R. China

[b.] College of Chemistry and Chemical Engineering, Hunan University of Arts and Science, Changde, 415000, P. R. China

[c.] LiFun Tech. Co. Ltd, Zhuzhou, 412000, P.R. China

E-mail: wanghy419@csu.edu.cn, haijun.peng@csu.edu.cn; zhaole@csu.edu.cn

1. Experimental section

1.1 Synthesis of UIO66-NH_2 and IL-UN66-NH_2

$ZrCl_4$ (≥99.9%, Aladdin) and 2-aminoterephthalic acid (98%, Macklin) (1:1 molar ratio) were weighed and added to a wide-mouth flask. Then 53 mL of N,N-dimethylformamide (DMF, 99.5%, Macklin) and 7 mL of glacial acetic acid (AR, Xihua) were added. The mixture was ultrasonicated for 30 min and stirred for 30 min to achieve complete dissolution, then transferred to a reactor and heated at 120 °C for 24 h. The products were washed three times with DMF/methanol mixture (4:1 volume ratio), followed by three washes with ethanol. Then they were dried overnight at 100 °C to obtain powdered UIO66-NH_2 (UN66). 0.3 g of sodium bis(trifluoromethylsulfonyl)imide (NaTFSI, Dodo Chemical Technology Ltd) was dissolved in 1 mL of 1-Ethyl-3-methylimidazolium bis(trifluoromethylsulfonyl)imide (EMIM, 99%, Macklin) ionic liquid, then thoroughly mixed UN66 with the prepared ionic liquid. The mixture was dried under vacuum in a glove box at 120 °C for 6 h to remove residual moisture, yielding IL-UN66-NH_2 (IL-UN66).

1.2 Preparation of solid polymer electrolyte membranes(SPEs)

IL-UN66 (5 wt% relative to NaTFSI) was weighed, followed by the addition of 3 mL acetone and 1 mL DMF to the glass bottle. The mixture was then ultrasonicated for 30 min to ensure complete and uniform dispersion. Subsequently, 0.4 g of NaTFSI was added into the glass bottle and stirred for 30 min until completely dissolved. Then 0.5 g of PVDF-HFP and 200 μL of FEC were introduced and stirred at 50 °C for 5 h until thoroughly dissolved, followed by slow stirring for 1 h and ultrasonicating for 5 min. The final mixture was coated with a squeegee and dried at 60 °C for 12 h. Following the same preparation steps without IL-UN66 yields the Base polymer solid

electrolyte membrane.

1.3 Preparation of $Na_4Fe_3(PO_4)_2(P_2O_7)$ (NFPP) cathode electrode

NFPP cathode powder, conductive carbon, and PVDF were weighed in a mass ratio of 8:1:1. A specified amount of NMP was added, and the mixture was thoroughly mixed and coated onto carbon-coated aluminum foil. Then dried overnight at 80 °C to obtain the NFPP cathode electrode.

1.4 Material characterization

The crystal structures of UN66 and SSEs were confirmed by powder X-ray diffraction (XRD, SmartLab 3kW, Rigaku Corporation) using Cu-Kα radiation. The specific surface area results were obtained using a Gas Sorption Analyzer (JW-BK200C-01). The microscopic morphology of the materials was observed using field emission scanning electron microscopy (FE-SEM, TESCAN MIRA3), while the elemental distribution of the samples was determined using energy dispersive spectroscopy (EDS, Bruker Quantax). Fourier transform infrared spectroscopy (FTIR) spectral measurements were conducted on a Thermo Scientific Nicolet iS50. Raman spectroscopy (Horiba LabRAM HR800) was collected using a laser 532 nm, 50 x microscope objective (Olympus, MLPlanTL N). X-ray photoelectron spectroscopy (XPS) was measured by an X-ray photoelectron spectroscopy (NEXSA, Thermo Fisher Scientific). Electron paramagnetic resonance (EPR) spectra (Bruker EMXplus) were collected at X-band (~9.85 GHz) microwave frequency using a Bruker ER 4122 SHQ resonator with 100 kHz magnetic field modulation. The data collection of the pouch cell is measured by the Neware battery test system.

1.5 Electrochemical analysis

The sodium ion transference number (t_{Na+}) of SPEs was measured at Multi Autolab/M204 by polarizing Na || SPEs || Na cells with a direct current voltage of 10 mV.

The t_{Na+} was calculated from Equation (1):

$$t_{Na^+} = \frac{I_S(\Delta V - I_0 R_0)}{I_0(\Delta V - I_S R_S)} \#(1)$$

where I_0 and R_0 are the initial current and interfacial resistance, I_S and R_S are the steady-state current and interfacial resistance, respectively, and ΔV presents the polarization voltage of 10 mV. Before measuring the ion transference number, we activated the sodium symmetric cell for 10 cycles at a current density of 0.1 mA cm^{-1} to achieve a relatively stable interface.

The electrochemical stability window of SPEs was measured by linear scanning voltammetry (LSV) of SS || SPEs || Na cells through a CHI660E electrochemical workstation, with a voltage range up to 6.0 V and a scan rate of 1 mV s^{-1}.

The electrochemical impedance spectra (EIS) of stainless steel (SS) SS || SPEs || SS cells were tested on a Multi Autolab/M204 to figure out the intrinsic resistance. The ionic conductivity (σ) was calculated from Equation (2):

$$\sigma = \frac{L}{R \times S} \#(2)$$

where L presents the thickness of SPE, R symbolizes the intrinsic resistance of the SPE in the EIS diagram, and S is the test area between SPE and the reference electrode of the cell.

The activation energy (E_a) was calculated from Equation (3):

$$\sigma = AT^{-\frac{1}{2}} \exp\left(\frac{-E_a}{T - T_0}\right) \#(3)$$

where T_0 presents the glass transition temperature, T symbolizes the absolute temperature, and *A* is the pre-exponential factor.

All coin cells were assembled in an argon-filled glove box. The cathode was prepared by coating aluminum foil with a slurry composed of commercial $Na_4Fe_3(PO_4)_2(P_2O_7)$ (NFPP). The

average mass loading of the active material was 2.5–3.0 mg cm^{-2}. The solid polymer electrode was sandwiched between the positive and negative electrodes to form the CR2016 button cell. Eelectrochemical cycling tests were conducted on the NFPP || SPEs || Na battery using a CT-3008 Neware testing system at 30 °C. The test voltage range was 1.5–3.8 V, with a current density of 1C = 110 mA g^{-1}. Simultaneously, NFPP || SPEs || Na batteries were assembled for rate testing at different current densities. Sodium symmetric cells were assembled and subjected to charge/discharge tests to evaluate the long-term cycling stability of the electrolyte and the reversible plating/stripping behavior of sodium. Prior to the tests, the cells were activated at a low current density of 0.05 mA cm^{-2}. For pouch cells, the cathode preparation followed the same process with an active material mass loading of 1.6 mg cm^{-2}. Pouch cells were fabricated by stacking the cathode and sodium foil (5.5 cm × 6 cm), placing them into a laminated pouch bag, and then vacuum sealing.

1.6 Calculation methods

All density functional theory (DFT) calculations were performed using the Vienna Ab-initio Simulation Package (VASP)[1]. The projector augmented wave (PAW) method[2] was utilized together with a plane-wave energy cutoff of 450 eV for treating the core-valence electron interactions. The electronic exchange and correlation effects were described by the generalized gradient approximation (GGA) with the Perdew-Burke-Ernzerhof (PBE) functional[3]. The Brillouin zone was sampled using the Monkhorst-Pack scheme with the k-point mesh density of less than 0.02 $Å^{-1}$. The energy convergence tolerance was set to below 1×10^{-5} eV for atomic position relaxation. Atomic positions were fully optimized until the maximal residual force was less than 0.05 $eVÅ^{-1}$. The binding energy (E_{bind}) was calculated according to the Equation (4),

$$E_{bind} = E_{12} - E_1 - E_2 \#(4)$$

where E_{12} is the total optimized energy of the complex structure, E_1, E_2 are the optimized energies of the isolated UN66 and sodium ions, respectively.

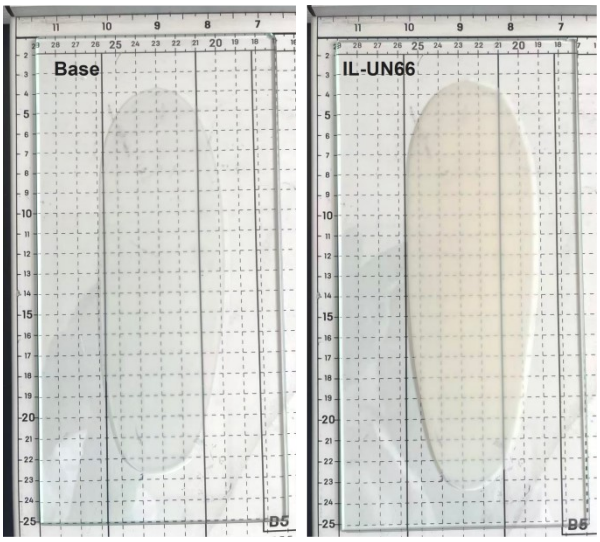

Fig. S1. Photographs of Base membrane and IL-UN66 membrane after heating 12 hours at 60°C in vacuum oven

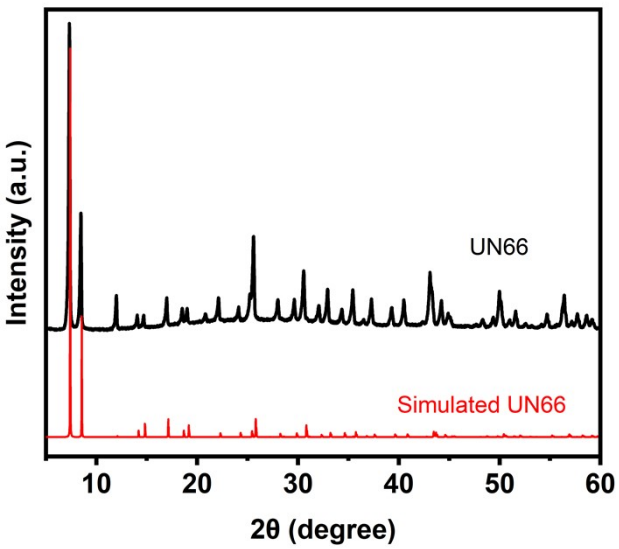

Fig. S2. XRD patterns of as-prepared UN66 and simulated UN66

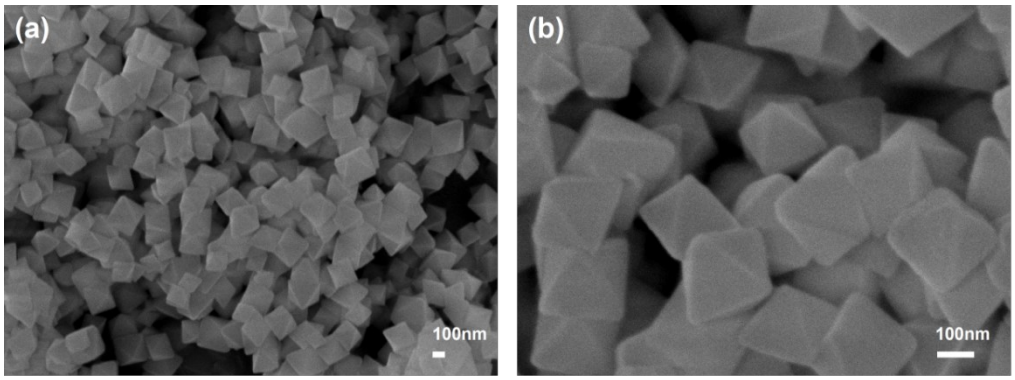

Fig. S3. SEM images of as-prepared UN66

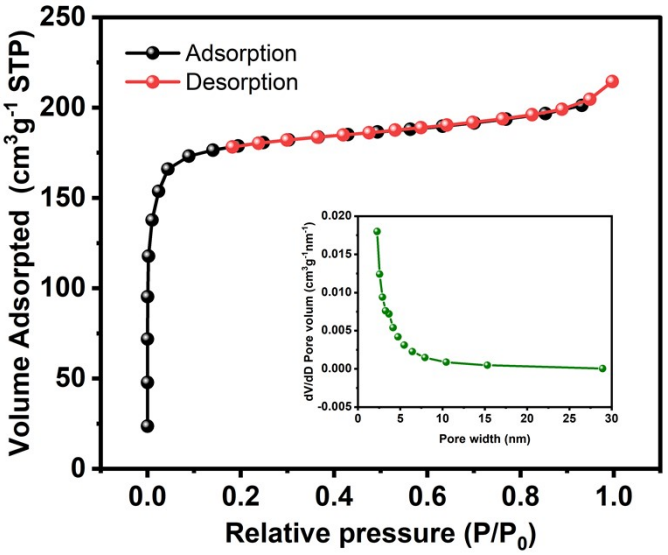

Fig. S4. Nitrogen adsorption-desorption isotherm and pore size distribution of UN66

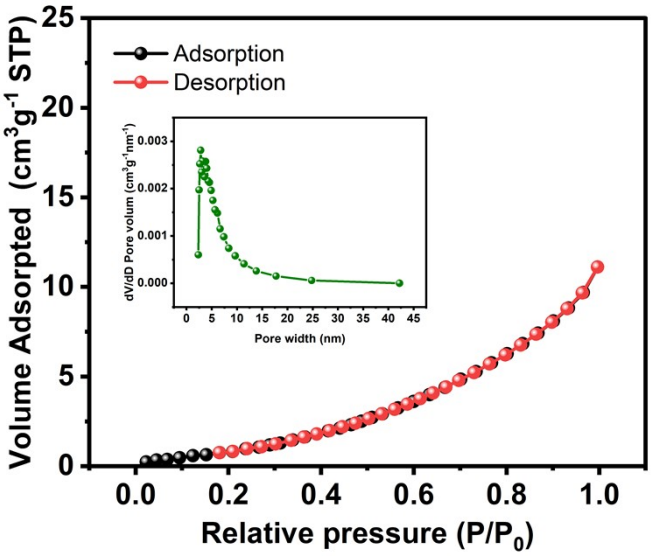

Fig. S5. Nitrogen adsorption-desorption isotherm and pore size distribution of IL-UN66

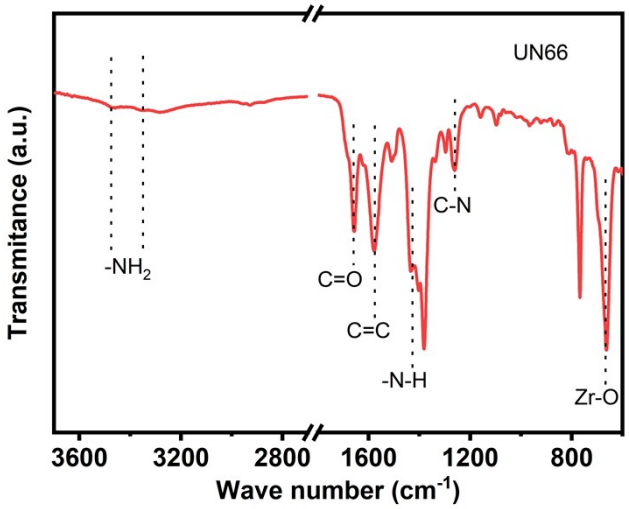

Fig. S6. FTIR spectrum of UN66

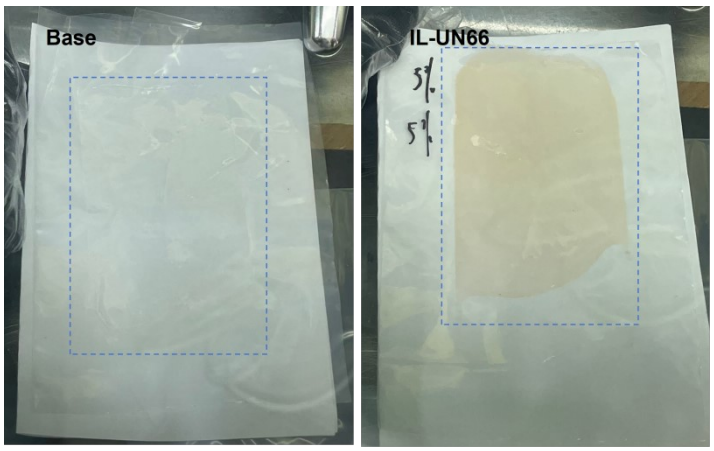

Fig. S7. Photographs of base and IL-UN66-containing polymer membranes

Fig. S8. Thickness photographs of the base and IL-UN66-containing polymer membranes

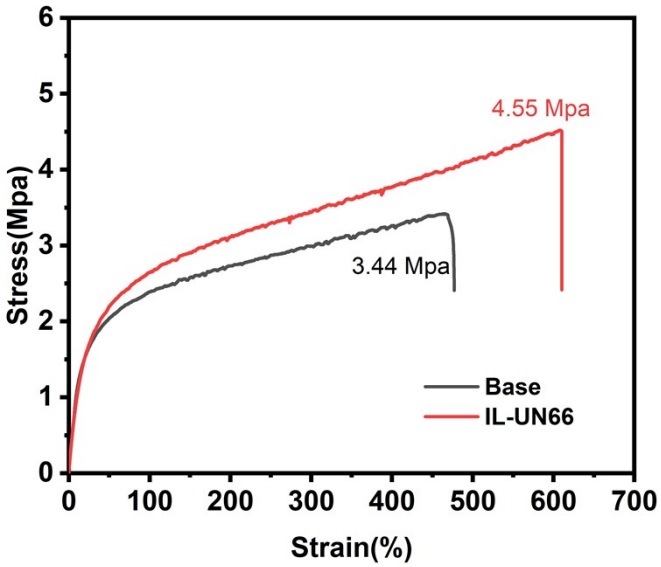

Fig. S9. Stress-strain curves of two membranes

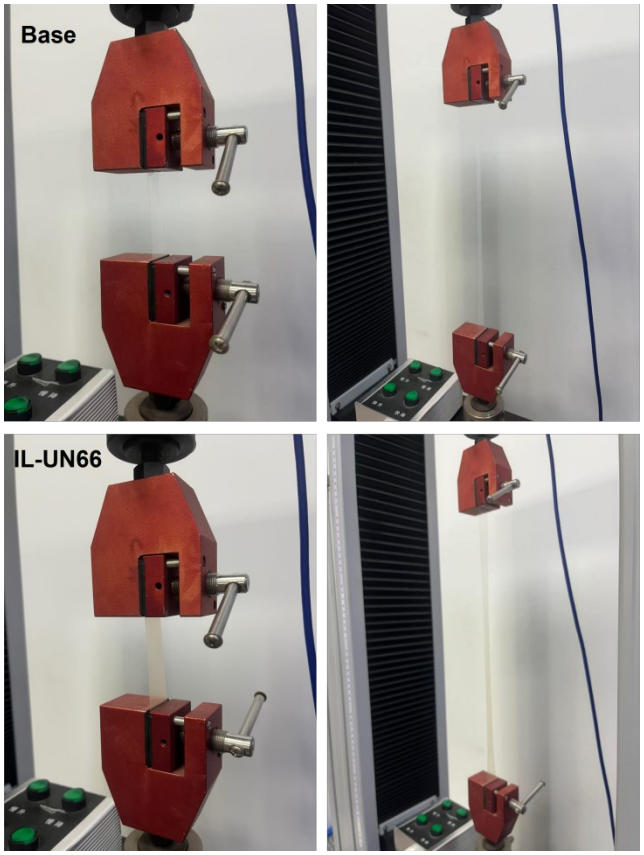

Fig. S10. Tensile strength test images of the base and IL-UN66 membranes

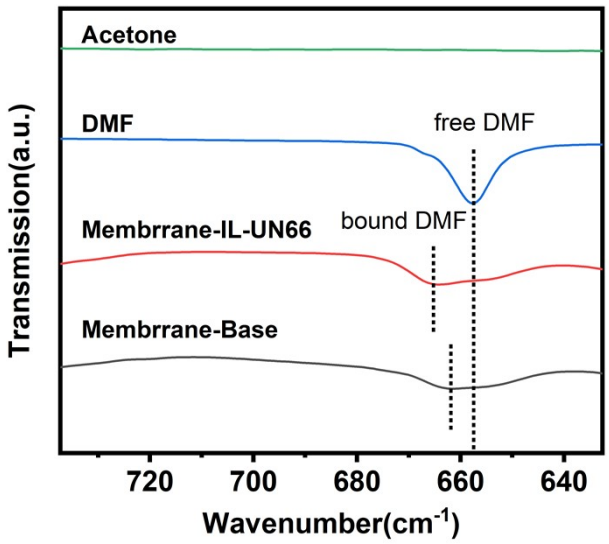

Fig. S11. Partial enlarged view of the FTIR spectrum (related to Figure 1d in the main text)

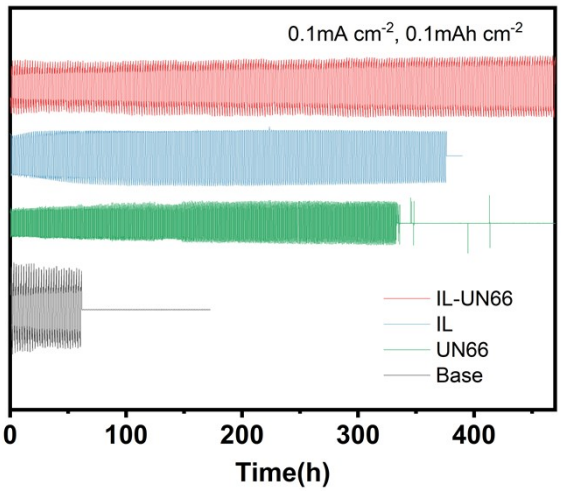

Fig. S12. The cycling performance of sodium symmetrical batteries(Base/UN66/IL/IL-UN66)

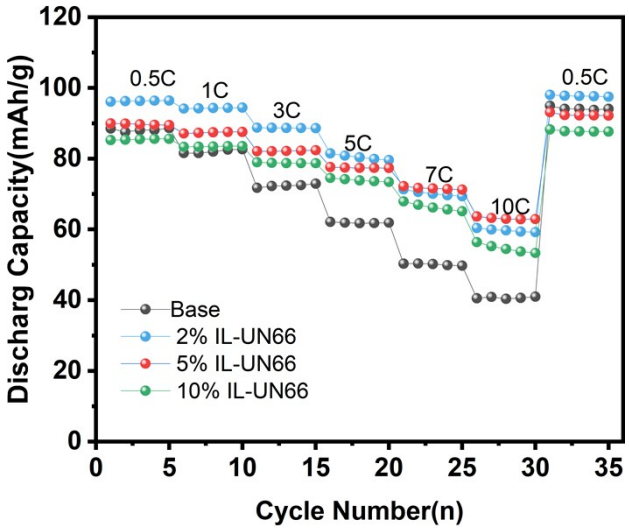

Fig. S13. The rate performance of NFPP|| SPEs||Na batteries(Base/UN66/IL/IL-UN66)

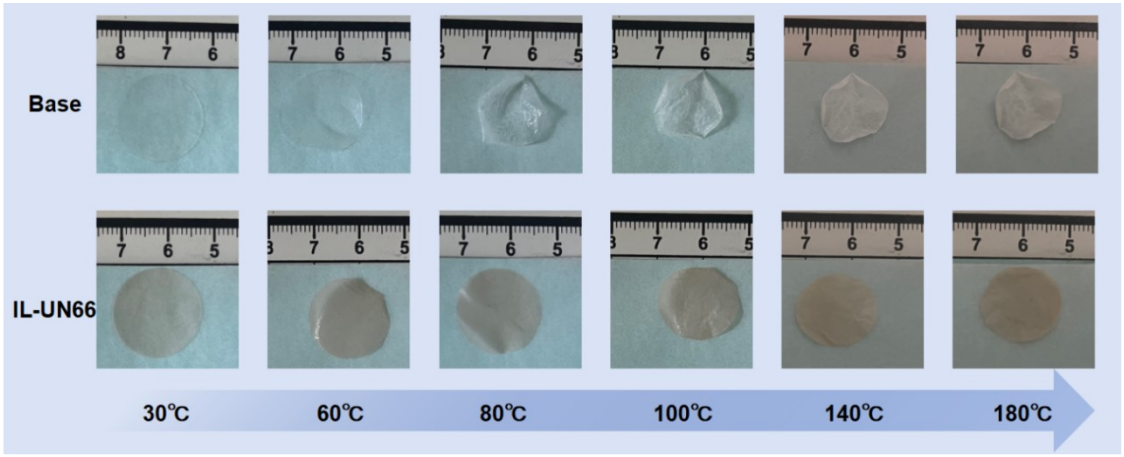

Fig. S14. Thermal shrinkage test of two membranes at different temperatures

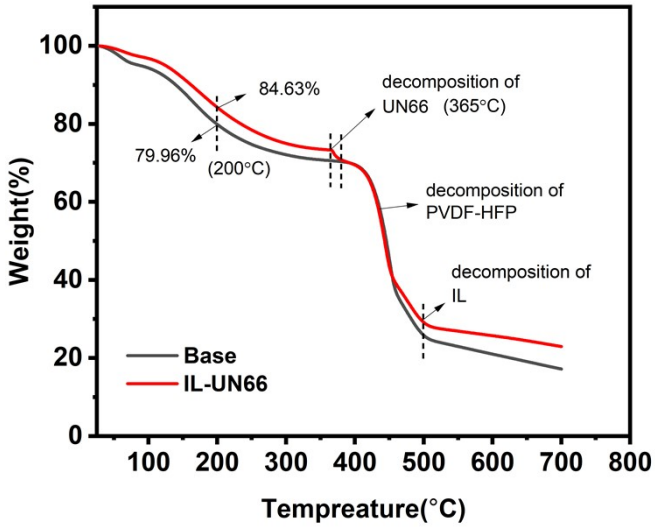

Fig. S15. TGA results of two membranes(Base/IL-UN66)

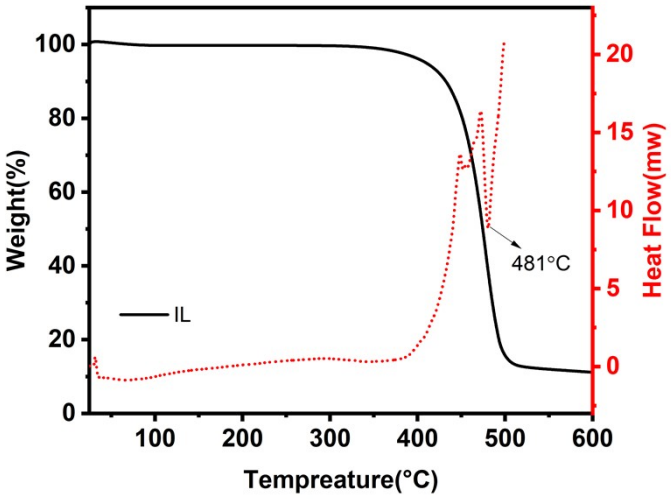

Fig. S16. TGA and DSC results of IL

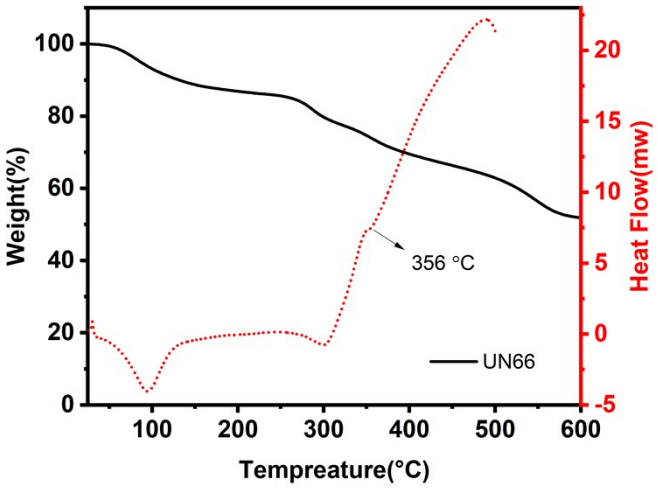

Fig. S17. TGA and DSC results of UN66

According to the analysis, the IL-UN66 membrane exhibits a weight loss of 15.37%, while the base membrane shows a weight loss of 20.04% at 200 °C, indicating that the incorporation of IL-UN66 improves the thermal stability of the membrane to a certain extent below 200 °C, which is consistent with the thermal shrinkage test results. Based on the TGA and DSC results of UN66 and IL alone, it is determined that UN66 undergoes thermal decomposition at 365 °C. According to existing literature reports, the thermal decomposition of PVDF-HFP occurs between 400-450 °C,[4,5] and IL is

almost completely degraded at 500 °C. It can be observed that at 700 °C, there is a difference in the final residual carbon content between the two membranes. The IL-UN66 membrane exhibits a higher residual carbon content, indicating a better char-forming ability, which may contribute to improved flame retardancy.[6,7]

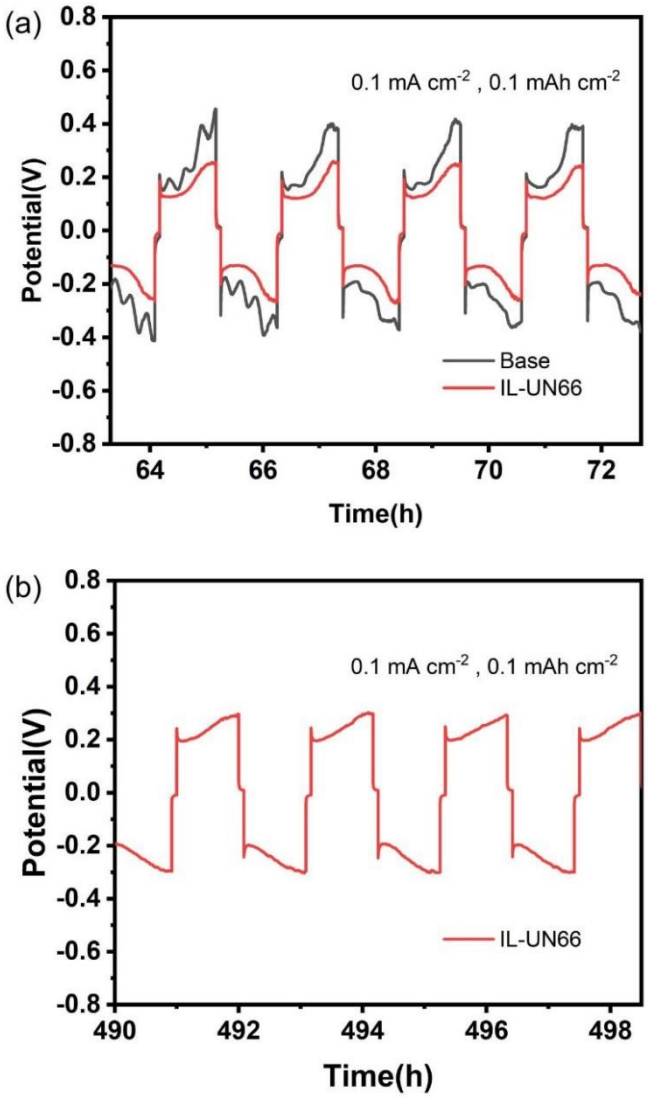

Fig. S18. Partial enlarged view of the cycling performance of sodium symmetrical batteries(related to Figure 4a in the main text)

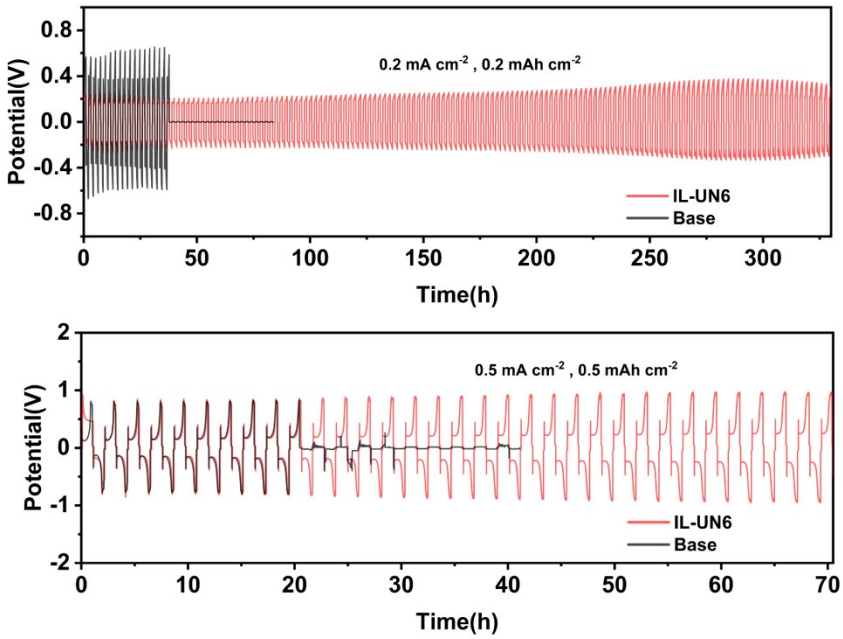

Fig. S19. The cycling performance of sodium symmetrical batteries at different current density

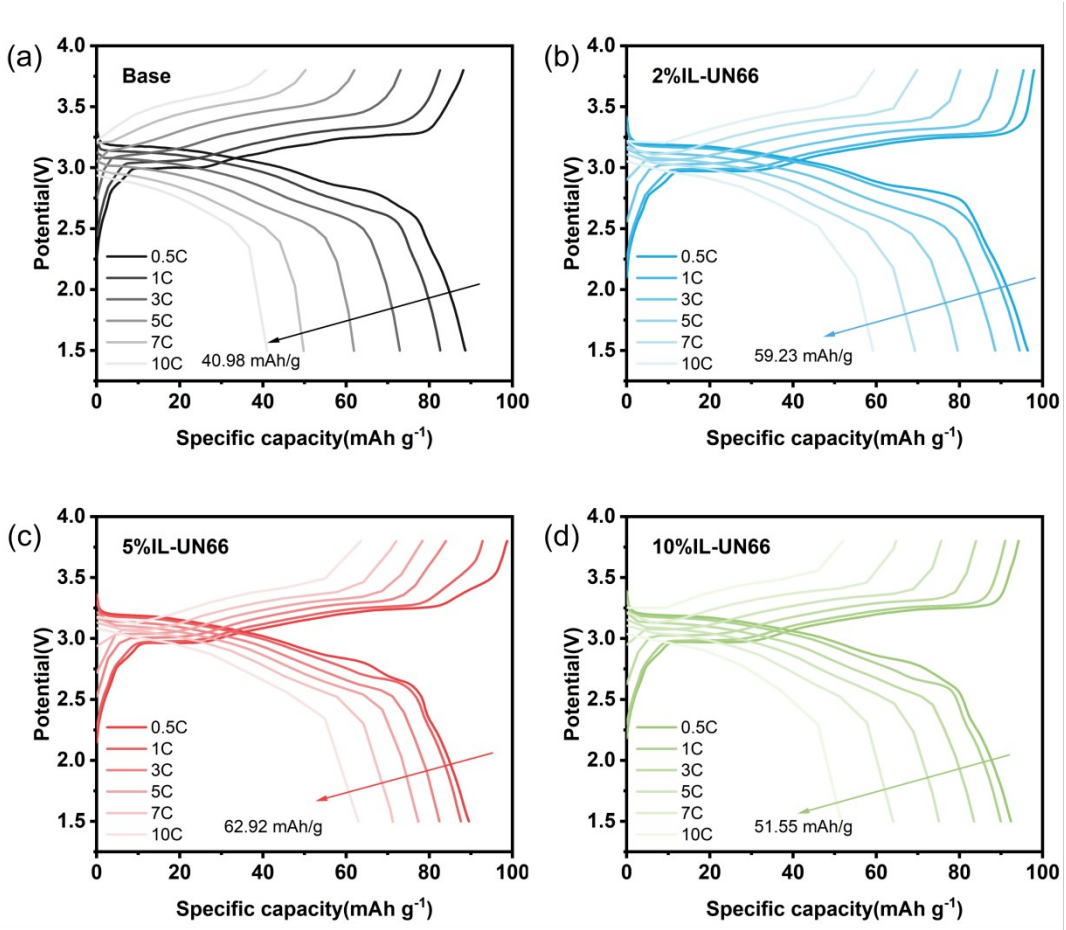

Fig. S20. Charge-discharge voltage profiles of (a) NFPP||Base SPEs||Na and (b) NFPP||2%/5%/10%IL-UN66 SPEs||Na cells at varied rates

References

[1] G. Kresse; J. Furthmüller. Efficient iterative schemes for ab initio total-energy calculations using a plane-wave basis set. *Phys. Rev. B.* 1996, **54**, 11169-11186.

[2] P.E. Blöchl. Projector augmented-wave method. *Phys. Rev. B.* 1994, **50**, 17953-17979.

[3] J.P. Perdew; K. Burke; M. Ernzerhof. Generalized gradient approximation made simple. *Phys. Rev. Lett.* 1996, **77**, 3865-3868.

[4] J. C. Barbosa, D. M. Correia, A. Fidalgo-Marijuan, R. Goncalves, S. Ferdov, V. D. Bermudez, S. Lanceros-Mendez and C. M. Costa, *ACS Appl. Mater. Interfaces*, 2023, **15**, 32301-32312.

[5] S. J. Tan, J. P. Yue, Z. Chen, X. X. Feng, J. Zhang, Y. X. Yin, L. Zhang, J. C. Zheng, Y. Luo, S. Xin and Y. G. Guo, *Energy Mater. Adv.,* 2024, **5**, e0076.

[6] M. Q. Shao, Y. Li, Y. R. Shi, J. T. Liu, B. X. Xue and M. Niu, *Polymers*, 2023, **15**, e2135.

[7] G. H. Yeoh, I. M. D. Cordeiro, W. Wang, C. Wang, A. C. Y. Yuen, T. B. Y. Chen, J. B. Vargas, G. Z. Mao, U. Garbe and H. T. Chua, *Adv. Mater.,* 2024, **36**, 54.